Research Article | Vol. 29, No. 14 / 5 July 2021 / Optics Express 21262
Optics EXPRESS

Effective-zero-thickness terahertz slot antennas using stepped structures

HYEONG SEOK YUN,[1,3] DUKHYUNG LEE,[1] AND DAI-SIK KIM[1,2,*]

[1]Department of Physics and Center for Atom Scale Electromagnetism, Ulsan National Institute of Science and Technology, Ulsan, 44919, Republic of Korea
[2]Department of Physics and Astronomy, Seoul National University, Seoul, 08826, Republic of Korea
[3]yoonhs1432@unist.ac.kr
[*]daisikkim@unist.ac.kr

Abstract: Metallic nanostructures play an essential role in electromagnetic manipulations due to the localization and enhancement of electromagnetic waves in nanogaps. Scaling down the dimensions of the gap, such as the gap width and the thickness, is an effective way to enhance light-matter interaction with colossal field enhancement. However, reducing the thickness below 10 nanometers still suffers from fabrication difficulty and unintended direct transmission through metals. Here, we fabricate effective-zero-thickness slot antennas by stepping metals in the vicinity of the gaps to confine electromagnetic waves in tiny volumes. We analyze and simulate terahertz transmission, and demonstrate the absorption enhancement of molecules in the slot antennas. Our fabrication technique provides a simple but versatile tool for maximum field enhancement and molecular sensing.

1. Introduction

Colossal electromagnetic enhancement occurs when light is highly squeezed in metallic nanostructures such as split-ring resonators, dipole, bowtie, slit, and slot antennas [1–14]. Among them, negative-type slot antennas are preferred for long-wavelength electromagnetic waves with the advantage of background-free transmission [15,16]. Many studies regarding slot antennas attempt to scale down the dimensions of the gap to achieve higher field enhancement, originating from large charge accumulation in the vicinity of the gap [15,17–21]. Recent developments in nano-fabrication techniques remarkably reduce the gap width down to 1 nanometer, achieving the field enhancement factors of 25,000 in the terahertz regime [6].

An alternative approach to increasing the field enhancement is to pare thick slot antennas down to 10 nm thickness by ion milling [22]. The reduction of the thickness lessens the effect of gap plasmon, a coupling of surface plasmons excited between metal-dielectric interfaces, increasing the field enhancement [6,23]. However, the fabrication of thin slot antennas below 10 nm thickness is still challenging.

In this paper, we realize effective-zero-thickness terahertz slot antennas by modifying the existing lithography technique. Stepping the bottom of each side of metals in the vicinity of the gap, the overlapped area between metals decreases, and the sharp edges of metals become closely adjacent. Consequently, the effect of gap plasmons significantly decreases, leading to maximized field enhancement.

2. Results and discussion

The schematics of the effective-zero-thickness slot antennas are illustrated in Fig. 1. A typical single slit is usually regarded as a one-dimensional structure from a distance (Fig. 1(a)). However, a close look shows it is a capacitor with a finite area (Fig. 1(b)) where gap plasmons can be excited. Field enhancement in the gap increases with a decrease of the gap width, but it is not the maximum value because the gap plasmons suppress field enhancement and make the

#427061 https://doi.org/10.1364/OE.427061
Journal © 2021 Received 14 Apr 2021; revised 9 Jun 2021; accepted 9 Jun 2021; published 22 Jun 2021

Optics EXPRESS

resonance red-shifted [22]. We solve the problem with effective-zero-thickness slot antennas simply by stepping the antennas, as shown in Fig. 1(c), which is analogous to line-type bowtie antennas operating with the background-free transmission, useful for the long-wavelength optical measurement with transmission geometry.

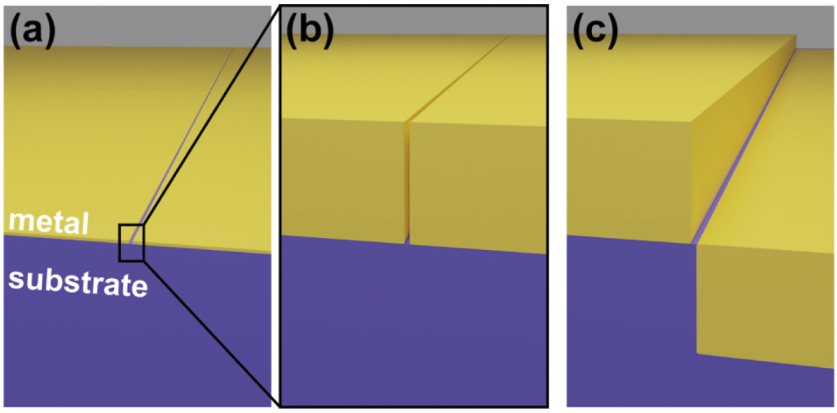

Fig. 1. Concept of stepped slot antennas. Schematics of one-dimensional-like antenna seen (a) from a distance and (b) close, and (c) stepped antenna with a one-dimensional gap.

We apply atomic layer lithography modified to realize the stepped structures [6,24]. First, we deposit a 5 nm thick titanium (Ti) and 100 nm thick gold (Au) film on a 500 μm thick silicon (Si) substrate. 300 nm thick vanadium (V) is patterned on the Ti/Au film in a rectangular shape by using photolithography (Fig. 2(a)). Here, V is selected as a mask layer because of its hardness against argon ion milling and vulnerability to chemical etching performed later. Au film is fully etched in a rectangular shape by ion milling at normal incidence, followed by partial etching of the Si substrate (Fig. 2(b)). A 5 nm thick alumina (Al_2O_3) spacer is conformally covered by atomic layer deposition (ALD) to define the gap width (Fig. 2(c)), and 100 nm thick Ti/Au is deposited again (Fig. 2(d)). Wet etching of the V layer completes the fabrication process, as

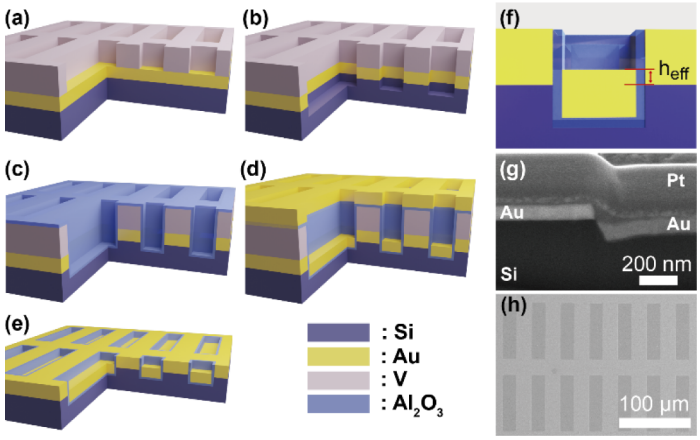

Fig. 2. Fabrication of the stepped slot antennas. (a)-(e) Schematics of the fabrication. (f) Schematics of h_{eff} across the gap. (g) Cross-sectional and (h) top-view SEM images. Platinum is deposited on the slot antennas to protect the nanostructures during focused ion beam milling.

Optics EXPRESS

illustrated in Fig. 2(e), confirmed in the cross-sectional scanning electron microscope (SEM) image in Fig. 2(g). Here, h_{eff} in Fig. 2(f) is defined as an overlapped height between each metal in the vicinity of the gap. We analyze cross-sectional SEM images to measure h_{eff}, which can be zero or even negative while keeping the thickness of metals constant. Perimeters of the terahertz antennas are 20 μm and 80 μm, respectively, for the resonance at the terahertz regime, as shown in the top-view SEM image in Fig. 2(h).

We perform terahertz time-domain spectroscopy (THz-TDS) to measure optical properties of the stepped slot antennas as shown in the schematics in Fig. 3(a) (see Supplement 1 for the fabrication detail). The polarization direction is perpendicular to the longer perimeters of the slot antennas (see Supplement 1 for the effect of the polarization parallel to long perimeters). To obtain the normalized amplitude, transmitted field amplitude through slot antennas is normalized by that through a Si substrate after applying fast Fourier transform (FFT) to the terahertz signals in time domain. Figure 3(b) shows the normalized amplitude with h_{eff} from 97 nm to 0 nm in the experiment. Here, h_{eff} of 97 nm indicates that the slot antennas are almost flat. We apply

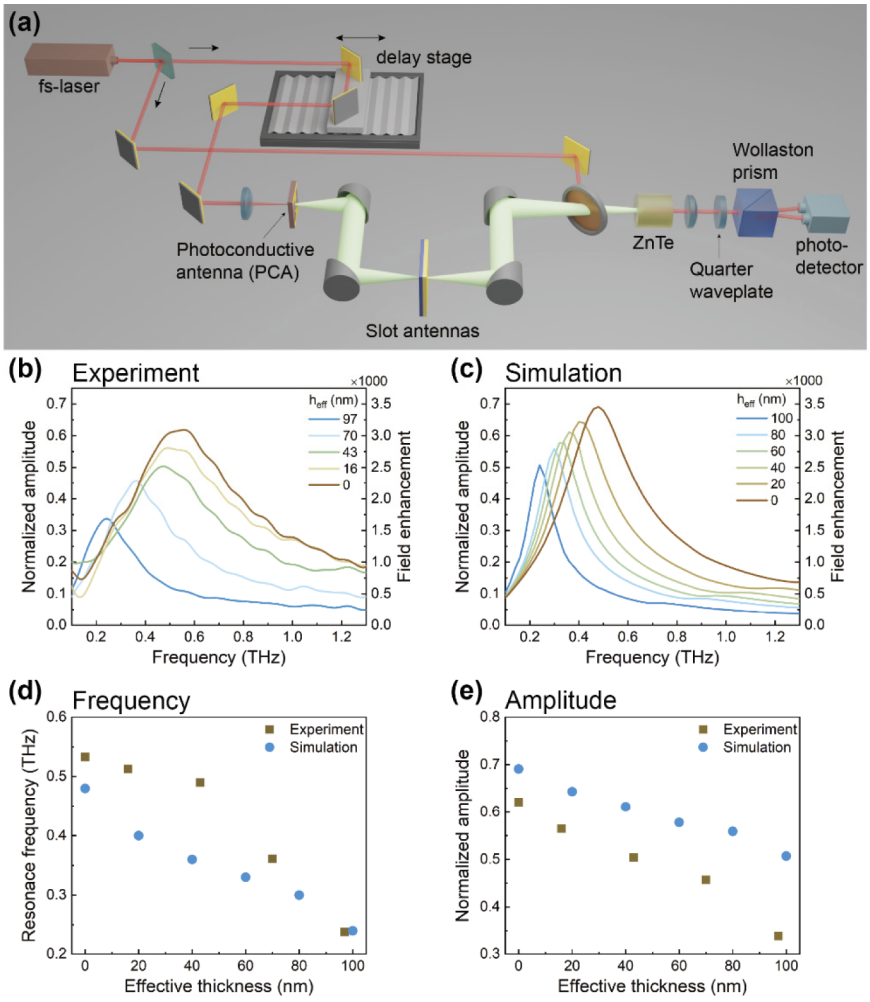

Fig. 3. Terahertz transmission measurements of the stepped slot antennas. (a) Schematics of THz-TDS setup. THz transmission spectra with h_{eff} from (b) the experiment and (c) the simulation. (d) The resonant frequency and (e) normalized amplitude with h_{eff}.

Optics EXPRESS

Kirchhoff integral formalism to extract and plot near-field enhancement in the gap denoted on the right side of the y-axis [25]. We conducted finite element method (FEM) simulation using commercial software (COMSOL Multiphysics 5.6, wave optics module) for a more comprehensive investigation. We applied the impedance boundary condition with a Drude model for the metal boundaries, considering the plasma frequency $\omega_p = 13.7$ PHz and the damping frequency $\gamma = 40.7$ THz. Refractive indexes for a Si substrate and an Al_2O_3 spacer used in the simulation are 3.4 and 2.1, respectively. The FEM simulation in Fig. 3(c) shows good agreement with the experimental results. The tendency of the resonant frequency and the normalized amplitude with respect to the h_{eff} is plotted in Fig. 3(d) and 3(e), respectively. The resonance frequencies are bule-shifted and normalized amplitudes are increased as the h_{eff} decreases, resulting from the release of the gap plasmons excited in the gap [22].

Cross-sectional field distribution clearly shows the advantages of the stepped slot antennas. For the slot antennas with the $h_{eff} = 100$ nm in Fig. 4(a), an electric field is uniformly distributed in the gap, and a weak fringe field is out of the gap. In Fig. 4(b) and Fig. 4(c), however, an electric field becomes spatially confined and enhanced in the overlapped volume with the h_{eff} reduced. The spatial confinements of the stepped slot antennas suggest that refractive index change in a very tiny volume is enough to modulate the overall optical response, as plotted in Fig. 4(d). In particular, even the fringe field confined out of the gap is useful for the accessibility of target molecules in hotspots, offering an excellent opportunity to be used for molecular detection [7,26–32]. This advantage is meaningful compared to previous work for the high-contrast refractive index sensing, which requires complicated processes like chemical etching and dilution [14].

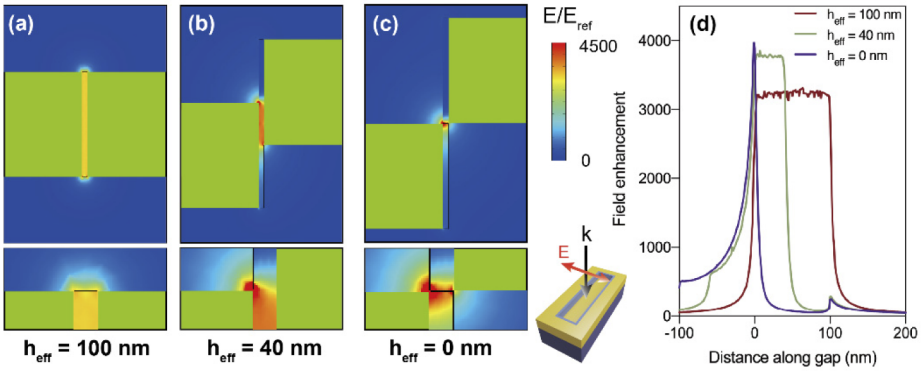

Fig. 4. Electric field distribution at the center of the longer perimeters of the stepped slot antennas. (a)-(c) Cross-sectional field distribution and (d) field enhancement along the gap with $h_{eff} = 100$ nm, 40 nm, and 0 nm, respectively. The schematic illustrates the propagation direction and polarization of the terahertz waves.

As a proof of concept for the application of the localized hotspot formed in the stepped slot antennas, we measure the absorption of water on the gap as water has a high absorption coefficient of $\sim 200\ cm^{-1}$ in the terahertz frequency regime [14]. We compare three cases of the slot antennas covered (1) with air, (2) with 100 nm thick water, and (3) with 20 μm thick water kept in a 20 μm thick polyimide (PI) spacer, as shown in the schematics in Fig. 5(a). In the cases (2) and (3), a Si substrate is capped on the antennas to seal a water layer (see Supplement 1 for the normalization in the case (1)). The normalized amplitude in the case (2) decreases by almost 35% compared to the case (1). Given that the absorption of the terahertz waves through a 100 nm thick water layer is negligible, the absorption may occur in a small volume near the gap. On the other hand, normalized amplitude in the case (3) decreases by 65% compared to the case

Optics EXPRESS

(1). The absorption in the case (3) is a sum of the absorption from the 5 nm thick hotspot and 20 μm thick bulk water. It is concluded in Fig. 5(b) that the absorption of the 5 nm thick water layer near the gap is similar to that of a 20 μm thick bulk water, demonstrating the absorption enhancement near the gap.

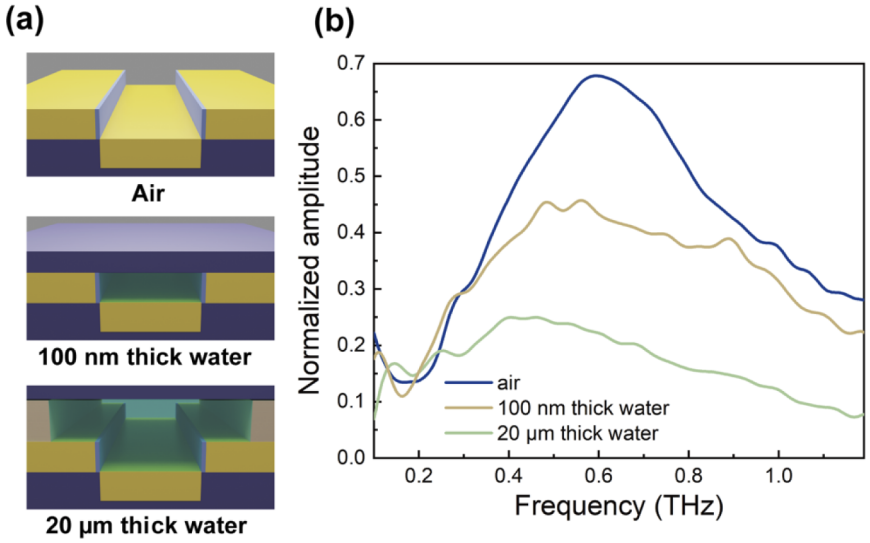

Fig. 5. Absorption enhancement of water. (a) Schematics and (b) transmission spectra of the slot antennas covered with air, 100 nm thick water layer, and 20 μm thick water layer, respectively.

For further quantitative analysis from the cases (2) and (3), we calculate the absorption coefficient of water at terahertz frequency via the Beer-Lambert law [7], $I = T^2 = e^{-\alpha d}$, where I is the transmitted intensity, T is the relative transmission, α is the absorption coefficient and d is the effective thickness of water layer. T in the cases (2) and (3) is normalized by that in the case (1). d in the case (2) is set to be 5 nm because the fringe field area is on the same scale as the gap width. d in the case (3) is the same as a 20 μm PI spacer thickness. We calculate $\alpha = -\left(\frac{2}{d}\right) ln(T)$ from the Beer-Lambert law, resulting in α_2 of 1,741,636 cm^{-1} for the case (2) and α_3 of 1,002 cm^{-1} for the case (3). The absorption enhancement in the case (2) compared to the absorption of bulk water is calculated as 8,708, which is in the same order as the electric field enhancement near the gap, demonstrating the usefulness of the fringe field despite the existence of an alumina layer. The discrepancy between the absorption enhancement and the field enhancement may be due to accuracy in estimating the hotspot volume where an electric field is enhanced. It is noteworthy that in Fig. 5(a), the stepped structure itself can be used as a built-in spacer without further fabrication, which is typically post-fabricated for the experiments in fluidics.

3. Conclusion

In conclusion, we fabricate the stepped slot antennas resonant at terahertz frequency to achieve the maximized field enhancement and localize the hotspot in a tiny volume. From the THz-TDS measurement and the FEM simulation, the effect of gap plasmons is highly reduced as h_{eff} approaches zero. The resonant frequency is thus blue-shifted with the field enhancement of its maximum value. Experimental demonstration of the absorption enhancement of a water layer on the gap provides an efficient way to detect molecules in a smaller volume with considerable field

Optics EXPRESS

enhancement. Our works on designing the stepped slot antennas will be of value to any field for which localized hotspots are highly required, such as molecular sensing.

Funding. National Research Foundation of Korea (NRF-2015R1A3A2031768); Ulsan National Institute of Science and Technology (1.190055.01, 1.190109.01, 1.210006.01).

Acknowledgments. We thank Sung Ju Hong and Young-Mi Bahk for helpful discussion and Dohee Lee for sample fabrication. Part of this study has been performed using facilities at IBS center for Correlated Electron Systems, Seoul National University. We wish to express thanks to the staff of the Seoul National University SEM Facility (NCIRF).

Disclosures. The authors declare no conflicts of interest.

Data availability. Data underlying the results presented in this paper are not publicly available at this time but may be obtained from the authors upon reasonable request.

Supplemental document. See Supplement 1 for supporting content.

References

1. T. W. Ebbesen, H. J. Lezec, H. F. Ghaemi, T. Thio, and P. A. Wolff, "Extraordinary optical transmission through sub-wavelength hole arrays," Nature **391**(6668), 667–669 (1998).
2. P. Mühlschlegel, H.-J. Eisler, O. J. F. Martin, B. Hecht, and D. W. Pohl, "Resonant Optical Antennas," Science **308**(5728), 1607–1609 (2005).
3. H. T. Miyazaki and Y. Kurokawa, "Squeezing visible light waves into a 3-nm-thick and 55-nm-long plasmon cavity," Phys. Rev. Lett. **96**(9), 097401 (2006).
4. A. Kinkhabwala, Z. Yu, S. Fan, Y. Avlasevich, K. Müllen, and W. E. Moerner, "Large single-molecule fluorescence enhancements produced by a bowtie nanoantenna," Nat. Photonics **3**(11), 654–657 (2009).
5. F. J. Garcia-Vidal, L. Martin-Moreno, T. W. Ebbesen, and L. Kuipers, "Light passing through subwavelength apertures," Rev. Mod. Phys. **82**(1), 729–787 (2010).
6. X. Chen, H. R. Park, M. Pelton, X. Piao, N. C. Lindquist, H. Im, Y. J. Kim, J. S. Ahn, K. J. Ahn, N. Park, D. S. Kim, and S. H. Oh, "Atomic layer lithography of wafer-scale nanogap arrays for extreme confinement of electromagnetic waves," Nat. Commun. **4**(1), 2361 (2013).
7. H. R. Park, K. J. Ahn, S. Han, Y. M. Bahk, N. Park, and D. S. Kim, "Colossal absorption of molecules inside single terahertz nanoantennas," Nano Lett. **13**(4), 1782–1786 (2013).
8. J. S. Ahn, T. Kang, D. K. Singh, Y. M. Bahk, H. Lee, S. B. Choi, and D. S. Kim, "Optical field enhancement of nanometer-sized gaps at near-infrared frequencies," Opt. Express **23**(4), 4897–4907 (2015).
9. T. Kang, J. Rhie, J. Park, Y.-M. Bahk, J. S. Ahn, H. Jeon, and D.-S. Kim, "Resonance tuning of electric field enhancement of nanogaps," Appl. Phys. Express **8**(9), 092003 (2015).
10. K. Lee, J. Jeong, Y.-M. Bahk, J. Rhie, I.-K. Baek, B. J. Lee, Y. H. Kang, S. Hong, G.-S. Park, and D.-S. Kim, "Microwave Funneling through Sub-10 nm Nanogaps," ACS Photonics **3**(4), 537–542 (2016).
11. N. Kim, S. In, D. Lee, J. Rhie, J. Jeong, D.-S. Kim, and N. Park, "Colossal Terahertz Field Enhancement Using Split-Ring Resonators with a Sub-10 nm Gap," ACS Photonics **5**(2), 278–283 (2018).
12. H. S. Yun, J. Jeong, D. Kim, and D. S. Kim, "Active Thermal Control of 5 nm Gap Terahertz Antennas," Adv. Opt. Mater. **7**(3), 1800856 (2019).
13. M. Runge, D. Engel, M. Schneider, K. Reimann, M. Woerner, and T. Elsaesser, "Spatial distribution of electric-field enhancement across the gap of terahertz bow-tie antennas," Opt. Express **28**(17), 24389–24398 (2020).
14. J. Jeong, H. S. Yun, D. Kim, K. S. Lee, H.-K. Choi, Z. H. Kim, S. W. Lee, and D.-S. Kim, "High Contrast Detection of Water-Filled Terahertz Nanotrenches," Adv. Opt. Mater. **6**(21), 1800582 (2018).
15. M. A. Seo, H. R. Park, S. M. Koo, D. J. Park, J. H. Kang, O. K. Suwal, S. S. Choi, P. C. M. Planken, G. S. Park, N. K. Park, Q. H. Park, and D. S. Kim, "Terahertz field enhancement by a metallic nano slit operating beyond the skin-depth limit," Nat. Photonics **3**(3), 152–156 (2009).
16. Y.-M. Bahk, D. J. Park, and D.-S. Kim, "Terahertz field confinement and enhancement in various sub-wavelength structures," J. Appl. Phys. **126**(12), 120901 (2019).
17. J. H. Kang, D. S. Kim, and Q. H. Park, "Local capacitor model for plasmonic electric field enhancement," Phys. Rev. Lett. **102**(9), 093906 (2009).
18. H. R. Park, S. M. Koo, O. K. Suwal, Y. M. Park, J. S. Kyoung, M. A. Seo, S. S. Choi, N. K. Park, D. S. Kim, and K. J. Ahn, "Resonance behavior of single ultrathin slot antennas on finite dielectric substrates in terahertz regime," Appl. Phys. Lett. **96**(21), 211109 (2010).
19. M. Shalaby, H. Merbold, M. Peccianti, L. Razzari, G. Sharma, T. Ozaki, R. Morandotti, T. Feurer, A. Weber, L. Heyderman, B. Patterson, and H. Sigg, "Concurrent field enhancement and high transmission of THz radiation in nanoslit arrays," Appl. Phys. Lett. **99**(4), 041110 (2011).
20. C. Feuillet-Palma, Y. Todorov, A. Vasanelli, and C. Sirtori, "Strong near field enhancement in THz nano-antenna arrays," Sci. Rep. **3**(1), 1361 (2013).
21. Y.-M. Bahk, S. Han, J. Rhie, J. Park, H. Jeon, N. Park, and D.-S. Kim, "Ultimate terahertz field enhancement of single nanoslits," Phys. Rev. B **95**(7), 075424 (2017).

Optics EXPRESS

22. D. Kim, J. Jeong, G. Choi, Y.-M. Bahk, T. Kang, D. Lee, B. Thusa, and D.-S. Kim, "Giant Field Enhancements in Ultrathin Nanoslots above 1 Terahertz," ACS Photonics **5**(5), 1885–1890 (2018).
23. S. Han, Y. M. Bahk, N. Park, and D. S. Kim, "Terahertz field enhancement in asymmetric and tapered nano-gaps," Opt. Express **24**(3), 2065–2071 (2016).
24. J. Jeong, J. Rhie, W. Jeon, C. S. Hwang, and D.-S. Kim, "High-throughput fabrication of infinitely long 10 nm slit arrays for terahertz applications," J. Infrared, Millimeter, Terahertz Waves **36**(3), 262–268 (2015).
25. J. S. Kyoung, M. A. Seo, H. R. Park, K. J. Ahn, and D. S. Kim, "Far field detection of terahertz near field enhancement of sub-wavelength slits using Kirchhoff integral formalism," Opt. Commun. **283**(24), 4907–4910 (2010).
26. H.-R. Park, X. Chen, N.-C. Nguyen, J. Peraire, and S.-H. Oh, "Nanogap-Enhanced Terahertz Sensing of 1 nm Thick (λ/106) Dielectric Films," ACS Photonics **2**(3), 417–424 (2015).
27. Y. G. Jeong, S. Han, J. Rhie, J. S. Kyoung, J. W. Choi, N. Park, S. Hong, B. J. Kim, H. T. Kim, and D. S. Kim, "A Vanadium Dioxide Metamaterial Disengaged from Insulator-to-Metal Transition," Nano Lett. **15**(10), 6318–6323 (2015).
28. H.-R. Park, S. Namgung, X. Chen, N. C. Lindquist, V. Giannini, Y. Francescato, S. A. Maier, and S.-H. Oh, "Perfect Extinction of Terahertz Waves in Monolayer Graphene over 2-nm-Wide Metallic Apertures," Adv. Opt. Mater. **3**(5), 667–673 (2015).
29. S. J. Park, S. A. N. Yoon, and Y. H. Ahn, "Dielectric constant measurements of thin films and liquids using terahertz metamaterials," RSC Adv. **6**(73), 69381–69386 (2016).
30. D.-K. Lee, H. Yang, H. S. Song, B. Park, E.-M. Hur, J. H. Kim, T. H. Park, and M. Seo, "Ultrasensitive terahertz molecule sensor for observation of photoinduced conformational change in rhodopsin-nanovesicles," Sens. Actuators, B **273**, 1371–1375 (2018).
31. S. H. Lee, D. Lee, M. H. Choi, J. H. Son, and M. Seo, "Highly Sensitive and Selective Detection of Steroid Hormones Using Terahertz Molecule-Specific Sensors," Anal. Chem. **91**, acs.analchem.9b01066 (2019).
32. Y. K. Srivastava, R. T. Ako, M. Gupta, M. Bhaskaran, S. Sriram, and R. Singh, "Terahertz sensing of 7 nm dielectric film with bound states in the continuum metasurfaces," Appl. Phys. Lett. **115**(15), 151105 (2019).